VIP Nanotransport Systems

DOI: 10.1002/anie.200603801

Supramolecular Aggregates of Dendritic Multishell Architectures as Universal Nanocarriers**

*Michał R. Radowski, Anuj Shukla, Hans von Berlepsch, Christoph Böttcher, Guillaume Pickaert, Heinz Rehage, and Rainer Haag**

The generation of nanocompartments for the homogeneous complexation and dissolution of active agents is an unsolved problem for many applications, for example, in catalysis, drug delivery, and ink formulation, among others. Supramolecular transport systems can be divided into two classes:[1] 1) physical aggregates of amphiphilic molecules,[2–4] such as vesicles or micelles and 2) covalently connected molecular architectures, so-called unimolecular transport systems.[5,6] A fundamental problem of all these carrier systems, however, is their limited matrix compatibility. They can either transport nonpolar molecules into an aqueous environment[7,8] or, if the system relies on an inverted micellar architecture, transfer polar molecules into a hydrophobic environment, such as an organic medium.[9,10] Therefore, the generation of nanocompartments that are compatible with various environments should solve many solubility and stability problems of active agents.

Herein we report on the design and properties of new multishell architectures based on hyperbranched polymeric cores surrounded by double-layered shells. This type of system can encapsulate and transport a wide variety of compounds ranging from nonpolar to ionic molecules in a broad matrix spectrum including nonpolar and polar organic as well as aqueous environments. In contrast to already existent micellar systems,[2,8,10] this new architecture mimics the structure of a liposome on a unimolecular basis (Figure 1). Liposomes are typically formed by self-association of amphiphilic molecules (for example, phospholipids) into bilayer vesicles that can solubilize polar chemical compounds in their aqueous interior.[4] Alternatively, they tend to encapsulate nonpolar guest molecules inside their bilayered hydrophobic wall.[11] Thus, by creating an analogous unimolecular architecture containing a hydrophobic middle layer, flanked by two hydrophilic domains, we expected liposome-like transport behavior with a higher stability.

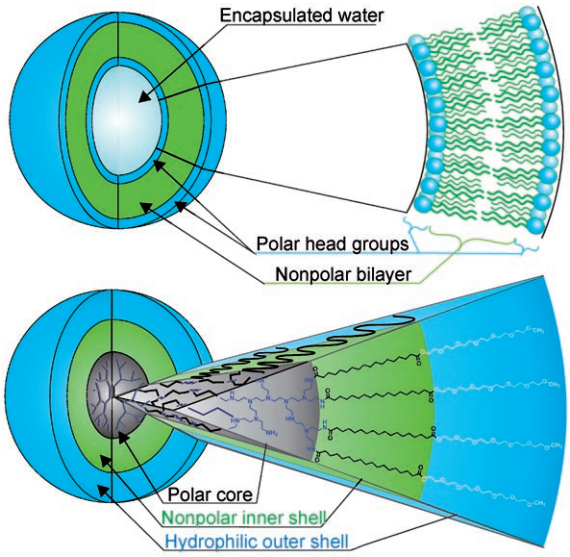

Figure 1. Schematic representation of a typical liposome structure (top) and the dendritic multishell architecture (bottom).

For the synthesis of such dendritic multishell architectures (Figure 1) a straightforward three-step synthesis was developed (Scheme 1).[12] We chose a modular approach for the assembly of cheap, commercially available building blocks: hyperbranched poly(ethylene imine) (PEI), dicarboxylic acids, and monomethyl poly(ethylene glycol) (mPEG). To understand the role of the individual domains (core, inner shell, outer shell) of these multishell architectures for the transport of guest molecules, we varied each individual part. Two PEI core molecules with different molecular weights ($M_n = 3600\ g\,mol^{-1}$, PD = 1.4; $M_n = 10\,500\ g\,mol^{-1}$, PD = 2.0) were chosen. These hyperbranched cores were functionalized with linear amphiphilic building blocks formed by alkyl diacids (C_6, C_{12}, or C_{18}) connected to monomethyl poly(ethylene glycol) (mPEG with 6, 10, and 14 glycol units on average) with different degrees of functionalization (70–100%).[13] The terminal mPEG chains acting as an external polar layer provide good solubility in water as well as in organic solvents and a high degree of biocompatibility.[14] The layer of long aliphatic chains is designed for the interaction with hydrophobic guest molecules inside the liposome-like structures, while the polar core as well as the outer polar shell

[*] M. R. Radowski, Dr. G. Pickaert, Prof. Dr. R. Haag
Institut für Organische Chemie und Biochemie
Freie Universität Berlin
Takustrasse 3, 14195 Berlin (Germany)
Fax: (+49) 30-838-53357
E-mail: haag@chemie.fu-berlin.de
Dr. A. Shukla, Prof. Dr. H. Rehage
Lehrstuhl für Physikalische Chemie II
Universität Dortmund
Otto-Hahn-Strasse 6, 44227 Dortmund (Germany)
Dr. H. von Berlepsch, Dr. C. Böttcher
Forschungszentrum für Elektronenmikroskopie
Freie Universität Berlin
Fabeckstrasse 36a, 14195 Berlin (Germany)

[**] R. H. thanks the German Science Ministry (BMBF) for a nanotechnology science award 03X5501A and M.R. is grateful to the Fonds der Chemischen Industrie for a PhD fellowship.

Supporting information for this article is available on the WWW under http://www.angewandte.org or from the author.

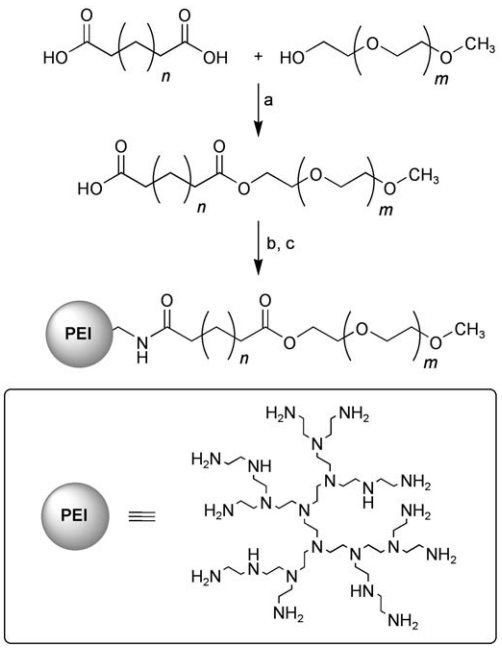

Scheme 1. Synthesis of dendritic multishell architectures: $PEI_x(C_{n+4}mPEG_{m+1})_{DF}$;[13] $n = 2$, 8, 14; $m \approx 5$, 9, 13. Reaction conditions: a) PTSA, toluene, reflux, 24 h, 70–85%; b) *N*-hydroxysuccinimide, *N*,*N*′-dicyclohexylcarbodiimide (DCC), THF, 0°C, 24 h, 93–97%; c) PEI, MeOH, RT, 24 h, 70–80% (50–65% after three steps). The depicted hyperbranched PEI structure shows a small idealized fragment of the actual polymer.

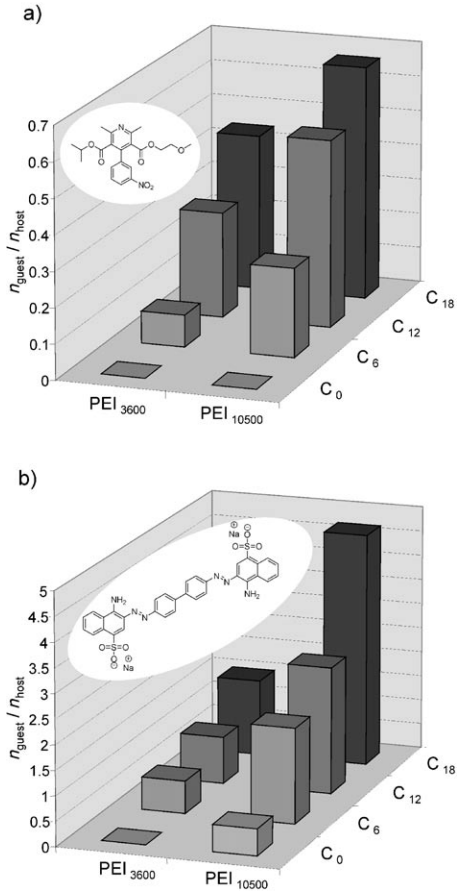

Figure 2. Transport–structure relationship with the changes of core size and diameter of the nonpolar inner shell (transport ratio n_{guest}/n_{host}) for a) nimodipine and b) congo red with $PEI_x(C_ymPEG_6)_{0.9}$ ($x = 3600$, 10500; $y = 0$, 6, 12, 18) polymers. No transport of nimodipine (< 0.1 mg L^{-1}) and congo red could be detected in the absence of the nanocarriers. For clarity reasons the error bars of the UV measurements are not shown; these deviations are typically in the range of ±10%.

offer a suitable environment for the incorporation of polar guest molecules. This modular approach combines a maximum of structural flexibility and an easy scale up of the process. The average molecular weights (M_n) of the dendritic multishell architectures can be adjusted between 10000 and 85000 g mol^{-1}, corresponding to theoretical particle diameters of 3–7 nm.

The versatile transport properties of these dendritic multishell architectures are demonstrated by using four different guest molecules in a wide polarity range of solvents: water, ethanol, chloroform, and toluene. As examples for hydrophobic drugs and dyes we used the calcium antagonist nimodipine ($M = 418.4$ g mol^{-1}; Figure 2a) and β-carotene ($M = 536.9$ g mol^{-1}). As representatives of polar guest molecules congo red ($M = 696.7$ g mol^{-1}, Figure 2b) and vitamin B_6 monohydrochloride ($M = 206.5$ g mol^{-1}) were chosen. Also several other hydrophobic and hydrophilic guest molecules such as vitamin A, vitamin D_3, vitamin B_2, and rose bengal were encapsulated and analyzed. Despite their different polarity and structure all guest molecules could be easily solubilized in their respective nonsolvents by PEI_{3600}-$(C_{18}mPEG_6)_{0.7}$ as the dendritic multishell nanocarrier.[12]

Additionally, a quantitative structure–transport relationship was established. While the size of the biocompatible mPEG shell had only a limited effect on the transport capacity (n_{guest}/n_{host} ratio increased by a factor of 1.5 from $mPEG_6$ to $mPEG_{14}$), the size of the polar core and the length of the nonpolar inner shell showed a significant effect on the transport of hydrophilic and hydrophobic guest molecules. The effects of the core and inner shell can be impressively shown by using the hydrophobic drug nimodipine in water (Figure 2a) and polar dye congo red in chloroform (Figure 2b). The encapsulation of polar molecules (congo red) was improved significantly by enlarging the core size for $PEI_x(C_{18}mPEG_6)_{0.9}$. The transport ratio ($n_{guest}/n_{host}$) was increased from 1.5:1 for PEI_{3600} to 4.7:1 for PEI_{10500}. This effect was less pronounced but still significant (up to a factor of two) for the transport of nonpolar guests such as nimodipine and β-carotene. More importantly, the role of the hydrophobic inner shell is essential for the encapsulation of nonpolar molecules. No transport of nimodipine (Figure 2a) was observed in the absence of the aliphatic inner shell. The encapsulation of nimodipine increases with the length of the nonpolar domain (C_6 to C_{18}) by a factor of three. Surprisingly, this nonpolar segment also plays an important role in the transport of polar molecules as deduced from the increasing transport capacity of congo red with growing nonpolar chain length (C_6 to C_{18}) by a factor of two (Figure 2b). These universal transport properties for hydrophilic and hydrophobic guest molecules in both polar and

nonpolar solvents have, to the best of our knowledge, not been reported for any other nanotransport system. Without further optimization this system can be generally applied and might solve many existing problems with nanocompartmentation and dissolution of active agents.

To better understand the underlying principles of this universal transport behavior, we investigated the structural aspects of the standard multishell nanotransporter, PEI_{3600}-$(C_{18}mPEG_6)_{0.7}$, in solution with and without guest molecules by three independent techniques: surface tension measurements, dynamic light scattering (DLS), and CryoTEM. The aggregation properties of the nanotransporters were analyzed over a wide concentration range from 0.002 $g\,L^{-1}$ (1.1×10^{-7} M) up to 4.0 $g\,L^{-1}$ (2.2×10^{-4} M) by surface-tension measurements, which were performed in a pendant drop apparatus. It turned out that the surface tension decreased linearly with the logarithm of the polymer concentration as suggested by the Gibbs adsorption isotherm (Figure 3). This trend implies that the dendritic multishell architectures in this respect do behave like amphiphilic compounds. In addition to the surface activity we could also determine a critical aggregation concentration (CAC) as shown in Figure 3. Above a characteristic concentration of 0.1 $g\,L^{-1}$ (for all studied polymers) the surface tension remains almost constant. This value corresponds to 10^{-7} to 10^{-5} M, which depends on the corresponding molar mass of the respective multishell polymer. In analogy to the critical micelle concentration (CMC) of surfactant solutions we can deduce that an aggregation process between individual dendritic multishell architectures ("unimers") takes place in solution. The extremely low CAC value points to a high stability of the supramolecular aggregates. This stability is in contrast to the classical picture of dendritic core-shell architectures, which are considered to act as unimolecular carrier systems.[1,9] Furthermore, the measured CAC is significantly lower than the CMC of typical ionic surfactants, such as potassium octadecanoate (CMC = 4.0×10^{-4} M),[15] or nonionic surfactants, such as alkyl-mPEGs (CMC range 10^{-3} to 10^{-5} M)[16] and many block copolymer micelles, such as pluronics (PPO-*b*-mPEG: CMC range 10^{-4} to 10^{-6} M).

To understand this aggregation phenomenon in detail, the transport capacities for congo red in chloroform and β-carotene in water were investigated as a function of the polymer concentration (Figure 3). Experiments performed with congo red in chloroform confirmed that transport only occurs when a threshold concentration of 0.1 $g\,L^{-1}$ is exceeded. The encapsulation of the dye can be directly observed by the accompanying color change (insert in Figure 3). At concentrations equal to or higher than 0.1 $g\,L^{-1}$ (6.0×10^{-6} M) the transport ratio n_{guest}/n_{host} was 1.5:1. This value varied only little upon increasing the polymer concentration up to 1.0 $g\,L^{-1}$ (2.5×10^{-5} M). For nonpolar molecules, such as β-carotene, a similar transport behavior was observed (Figure 3). The nonlinear changes in transport capacities of both polar and nonpolar guest molecules in water and organic solvents near the CAC support the previous finding that the dendritic multishell architectures do not act as unimolecular carrier systems. Instead, the measurements suggest that supramolecular aggregates are responsible for their transport ability.

We confirmed this hypothesis by DLS measurements (Figure 4a–c). DLS measurements above the CAC[17] were performed for $PEI_{3600}(C_{18}mPEG_7)_{0.7}$ in a range of different concentrations between 0.5 $g\,L^{-1}$ and 10.0 $g\,L^{-1}$ (3.0×10^{-5} M to 5.7×10^{-4} M) and resulted in diameters of approximately 5 nm (unimer) and 35 nm (aggregate) using a biexponential model for data evaluation. Molecular modeling[18] of the unimolecular dendritic multishell architecture, $PEI_{3600}(C_{18}mPEG_6)_{0.7}$, in a periodic water box gave a typical diameter of approximately 6 nm, which is in good agreement with the experimental value.[12]

In the DLS measurements in chloroform the scattering intensity of the aggregates is smaller than in water because of the close proximity of refractive indices of mPEG and chloroform (matching solvent conditions). Therefore, mPEG chains become undetectable in chloroform with the result that the aggregates appeared 15% smaller in chloroform (ca. 30 nm) than in water (ca. 35 nm; Figure 4a). Upon encapsulation of guest molecules a drastic change was observed in the size of the supramolecular aggregates. It is surprising that the size change does not depend on the polarity of the solvent and the guest molecules, but rather on the geometry of the latter. By encapsulation of linear molecules (congo red, β-carotene) the particle size increases from 35 nm to a diameter of approximately 120 nm in both solvents, water and chloroform (Figure 4c). For the more globular molecules nimodipine and vitamin B_6 the effects were opposite and gave

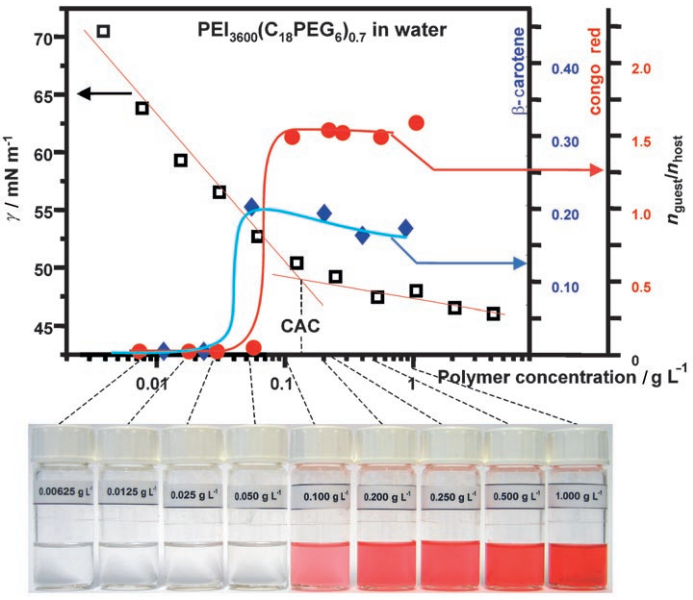

Figure 3. Surface tension as a function of the concentration for the standard multishell nanotransporter $PEI_{3600}(C_{18}mPEG_6)_{0.7}$ (□, left scale). The data allowed estimation of CAC value (CAC = 0.12 $g\,L^{-1}$, 6.5×10^{-6} M). Transport capacity concentration dependence for β-carotene (blue ◆) in water and congo red (red ●) in chloroform are summarized in the two right scales in n_{guest}/n_{host} ratio. The insert visualizes the congo red transport for different polymer concentrations.

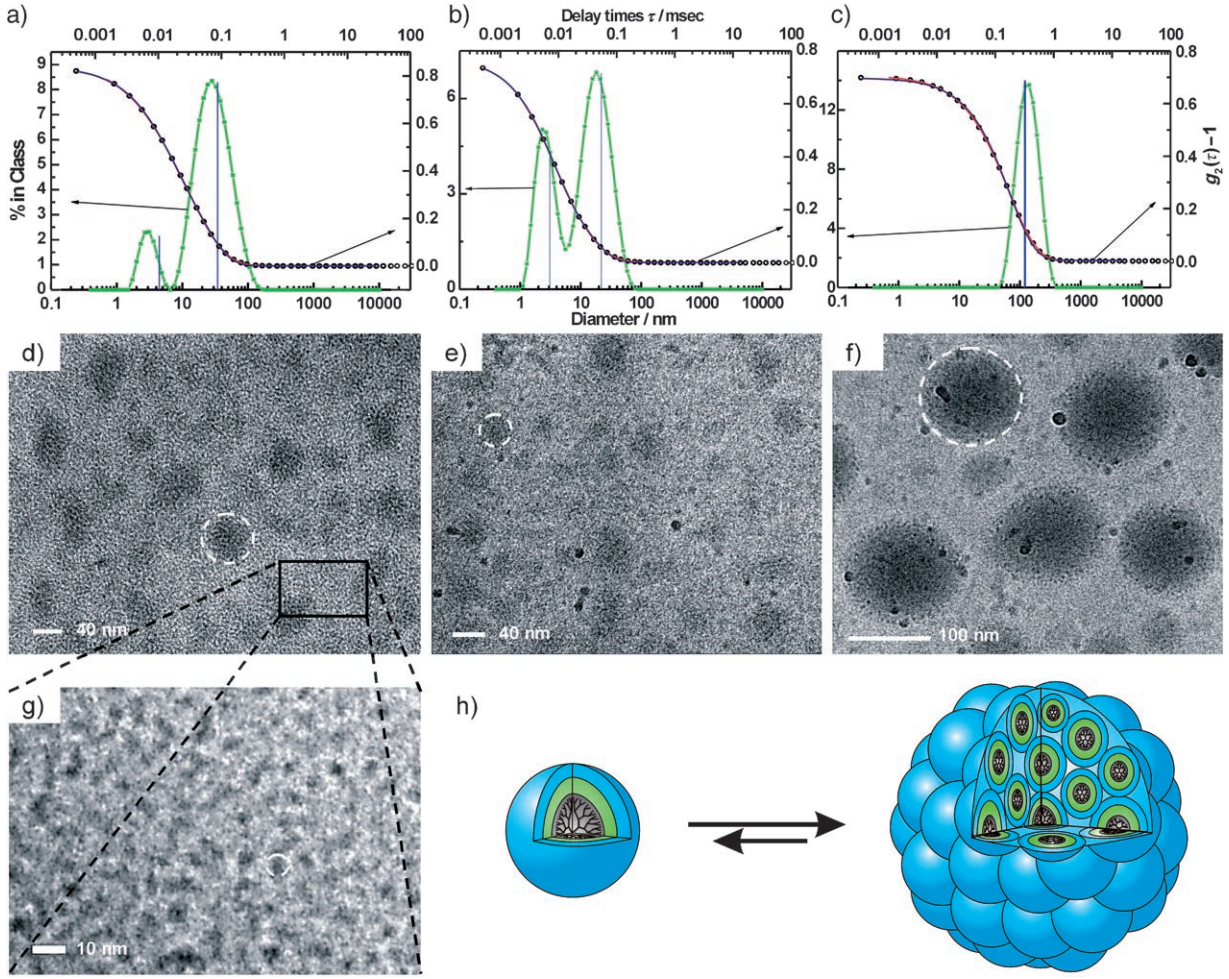

Figure 4. The size of the unimolecular multishell architecture, $PEI_{3600}(C_{18}mPEG_6)_{0.7}$, and its aggregates were determined by DLS (a–c) and CryoTEM (d–g) measurements. a) For the pure polymer diameters of aggregates were determined by DLS to 34.9 nm (with use of Laplace inversion, green curve) or 34.6 nm (biexponential, blue curve). b) The size of polymer aggregates with nimodipine were found to be 21.9 nm or 23.2 nm. c) For β-carotene–polymer aggregates diameters were determined to 144 nm or 121 nm. In addition to the aggregates, the "unimers" were observed by DLS and the diameters were determined to be about 5 nm (a, b). Because of the large dimensions of the β-carotene–polymer aggregates a detection of unimers was not possible in this case. All results from DLS were confirmed by CryoTEM measurements (d–g). The size of the unimers were determined to be about 5 nm. d) Aggregate diameters for pure multishell nanocarriers were determined in a range of 30–50 nm. e) After encapsulation of nimodipine the size changed to diameters of 20–30 nm. f) Encapsulation of β-carotene increased the size of aggregates to 110–130 nm. g) Enlargement from (d). h) Model of a unimer (left) and supramolecular aggregate (right). The concentration of all samples analyzed by CryoTEM and DLS was 1.0 $g\,L^{-1}$ of polymer in pure water (6×10^{-5} M).

assemblies of approximately 20 nm diameter in both solvents (Figure 4b). This observation may be a result of the fact that these molecules are preferentially located in the interfacial region and behave as "cosurfactants" that reduce the interfacial tension and thus prevent the formation of larger aggregates. In contrast, linear guest molecules might act as noncovalent linkers between the assemblies' constituents owing to their extended geometry (congo red,[19] β-carotene). All these supramolecular aggregates showed high stabilities, were detectable in solution for more than a year, and survived filtration procedures as well as size exclusion chromatography.[12]

The direct structural analyses of these supramolecular aggregates were performed by CryoTEM[20] measurements of $PEI_{3600}(C_{18}mPEG_7)_{0.7}$ at a concentration of 1.0 $g\,L^{-1}$, which is well above the CAC (Figure 4d–g). The CryoTEM micrographs revealed two coexisting types of objects for the dendritic multishell architecture in water. Small particles with a diameter of 4–6 nm were observed, which corresponds well to the size calculated for the standard unimolecular nanotransporter.[12] Additionally, larger spherical aggregates with diameters in the range of 30–50 nm (Figure 4d) were detected. In the presence of nimodipine as a guest molecule, CryoTEM measurements revealed a typical assembly size of 25–35 nm (Figure 4e), whereas with β-carotene the aggregate size increased dramatically to diameters of 120–140 nm (Figure 4f). Interestingly, the micrographs reveal a noticeable granular fine structure and a high contrast for the larger aggregates. The ultrastructural features are fundamentally different from the CryoTEM images of liposomes and micelles,[21] thus suggesting that the aggregates are indeed formed by a large number of "elementary" unimolecular

species. Interestingly, in those areas where these particles appear densely packed (Figure 4 g) the typical interparticle spacing does not fall below 8–9 nm. This finding is an indirect indication that an outer shell of the particles, which is obviously not visible in the images, prevents a denser packing. This feature can be proven by embedding the supramolecular aggregates in a matrix of heavy-metal salt (uranyl acetate), as is usually done for high contrast imaging in TEM. The total diameter of the particles becomes visible and amounts to the expected value of 8–9 nm.[12] Also, the apparent size-controlling capability of the guest molecules from CryoTEM measurements coincides with the DLS data (Figure 4 a–c). We assume that the self-assembly process depends on the presence of long aliphatic chains in the molecular structure. As was demonstrated in Figure 2 only polymers with nonpolar domains could efficiently transport guest molecules of both polar and nonpolar types. We can conclude that intra- and intermolecular interaction between aliphatic chains allows the creation and stabilization of aggregates in solution. Additionally, the presence of poly(ethylene glycol) chains might also play an important role[22] for the stabilization of these aggregates.

In conclusion, these new supramolecular aggregates are fundamentally different in their structure and transport behavior as compared to simple detergent micelles and unimolecular carrier systems reported previously.[5,9,23] The experiments described above clearly demonstrate that the multishell nanocarriers self-assemble into supramolecular aggregates above a well-defined threshold concentration (CAC). In addition, this new type of supramolecular aggregate only acts as a carrier for guest molecules after self-assembly and not as unimolecular systems. Surprisingly, the multishell nanocarrier aggregates not only can accommodate polar and nonpolar guest molecules but can also adapt to various environmental polarity conditions ranging from toluene to water. Based on this universal transport behavior, they can be considered as "chemical chameleons". This new universal nanocarrier system is versatile and could potentially be used for the transport of different guest molecules such as drugs, dyes, toxic compounds, stabilizers, metal nanoparticles, and fluorescent markers, and is therefore of interest for a number of biomedical and technological applications.

Received: September 15, 2006

Keywords: core-shell structures · dendritic polymers · drug delivery · nanomaterials · supramolecular chemistry

[1] R. Haag, *Angew. Chem.* **2004**, *116*, 280 – 284; *Angew. Chem. Int. Ed.* **2004**, *43*, 278 – 282.
[2] a) K. Kataoka, A. Harada, Y. Nagaski, *Adv. Drug Delivery Rev.* **2001**, *47*, 113 – 131; b) D. E. Discher, A. Eisenberg, *Science* **2002**, *297*, 967 – 973.
[3] N. Nishiyama, K. Kataoka, *Adv. Polym. Sci.* **2006**, *193*, 67 – 101.
[4] a) D. D. Lasic, D. Needham, *Chem. Rev.* **1995**, *95*, 2601 – 2628; b) D. C. Drummond, M. Zignani, J.-C. Leroux, *Prog. Lipid Res.* **2000**, *39*, 409 – 460.
[5] a) M. M. Conn, J. J. Rebek, *Chem. Rev.* **1997**, *97*, 1647 – 1668; b) M. W. P. L. Baars, E. W. Meijer, *Top. Curr. Chem.* **2000**, *210*, 131 – 182.
[6] a) C. C. Lee, J. A. MacKay, J. M. J. Fréchet, F. C. Szoka, Jr., *Nat. Biotechnol.* **2005**, *23*, 1517 – 1526; b) U. Gupta, H. B. Agashe, A. Asthana, N. K. Jain, *Biomacromolecules* **2006**, *7*, 649 – 658.
[7] a) G. R. Newkome, C. N. Moorefield, G. R. Baker, M. J. Saunders, S. H. Grossman, *Angew. Chem.* **1991**, *103*, 1207 – 1209; *Angew. Chem. Int. Ed. Engl.* **1991**, *30*, 1178 – 1180; b) G. Chen, Z. Guan, *J. Am. Chem. Soc.* **2004**, *126*, 2662 – 2663.
[8] R. Savic, L. Luo, A. Eisenberg, D. Maysinger, *Science* **2003**, *300*, 615 – 618.
[9] J. F. G. A. Jansen, E. M. M. de Brabander-van den Berg, E. W. Meijer, *Science* **1994**, *266*, 1226 – 1229.
[10] a) S. Stevelmans, J. C. M. van Hest, J. F. G. A. Jansen, D. A. F. J. van Boxtel, E. M. M. de Brabander-van den Berg, E. W. Meijer, *J. Am. Chem. Soc.* **1996**, *118*, 7398 – 7399; b) M. Krämer, J.-F. Stumbé, H. Türk, S. Krause, A. Komp, L. Delineau, S. Prokohorova, H. Kautz, R. Haag, *Angew. Chem.* **2002**, *114*, 4426 – 4431; *Angew. Chem. Int. Ed.* **2002**, *41*, 4252 – 4256.
[11] A. W. K. Ng, K. M. Wasan, G. Lopez-Berestein, *Methods Enzymol.* **2005**, *391*, 304 – 313.
[12] For additional information on materials, synthetic procedure, and methods, see the Supporting Information.
[13] For the nomenclature of the standard polymer we use the abbreviation $PEI_{3600}(C_{18}mPEG_6)_{0.7}$, with the numbers indicating the respective core molecular weight M_n, the inner shell carbon chain length, the outer PEG shell number of glycol units, and the degree of functionalization of the terminal NH_2 groups.
[14] a) J. M. Harris, R. B. Chess, *Nat. Rev. Drug Discovery* **2003**, *2*, 214 – 221; b) T. So, H.-O. Ito, Y. Tsujihata, M. Hirata, T. Ueda, T. Imoto, *Protein Eng.* **1999**, *8*, 701 – 705.
[15] K. Shinoda, *J. Phys. Chem.* **1956**, *60*, 1439 – 1441.
[16] I. Reif, M. Mulqueen, D. Blankschtein, *Langmuir* **2001**, *17*, 5801 – 5812.
[17] The size of the unimers could not be determined below the CAC because the low scattering intensity prevented a reliable estimation.
[18] Method: HyperChem 6.0 (Hypercube, Inc., USA).
[19] M. Shibayama, F. Ikkai, R. Moriwaki, S. Nomura, *Macromolecules* **1994**, *27*, 1738 – 1743.
[20] M. Adrian, J. Dubochet, J. Lepault, A. W. McDowall, *Nature* **1984**, *308*, 32 – 36.
[21] G. A. F. v. Tilborg, W. J. M. Mulder, N. Deckers, G. Storm, C. P. M. Reutelingsperger, G. J. Strijkers, K. Nicolay, *Bioconjugate Chem.* **2006**, *17*, 741 – 749.
[22] D. Yan, Y. Zhou, J. Hou, *Science* **2004**, *303*, 65 – 67.
[23] M. W. P. L. Baars, R. Kleppinger, M. H. J. Koch, S.-L. Yeu, E. W. Meijer, *Angew. Chem.* **2000**, *112*, 1341 – 1344; *Angew. Chem. Int. Ed.* **2000**, *39*, 1285 – 1288.

